BSGF - Earth Sciences Bulletin 2023, 194, 16

https://doi.org/10.1051/bsgf/2023011

BSGF Earth Sciences Bulletin

Available online at:
www.bsgf.fr

OPEN ACCESS

First report of an Ediacarian basement in the Western Alps: the Serre Chevalier crystalline unit (Briançonnais domain, France)

Denis Thiéblemont[1,*], Jean-Baptiste Jacob[2], Philippe Lach[1], Catherine Guerrot[1] and Mathieu Leguérinel[1]

[1] BRGM, B.P. 6009, 45060 Orléans Cedex, France
[2] The Njord Centre, Department of Geoscience, University of Oslo, Oslo, Norway

Received: 14 April 2023 / Accepted: 11 September 2023 / Publishing online: 20 December 2023

Abstract – We report new LA-ICP-MS U-Pb zircon ages of varied crystalline rocks occurring in the Serre Chevalier crystalline terrain, an allochtonous basement unit located at the top of the Briançonnais nappes stack ~5 km west of Briançon city. Mapped as an undifferentiated metasedimentary basement on the geological map at 1/50,000 scale, this unit actually displays varied lithologies including alternating micaschist, paragneiss, quartzite, coarse-grained conglomerate and felsic (leptynite) to mafic (amphibolite) gneiss of magmatic origin. All rocks were metamorphosed in response to a dominant pre-Alpine event under amphibolite facies conditions. Partial recrystallization under low-grade amphibolite to greenschist facies conditions was associated with alpine events. Zircon ages were obtained on four types of rocks: (i) a micaceous quartzite from the core of the metasedimentary unit displays a dominant age population around 610 Ma, with a minimal age of 580 Ma, and subordinated age populations at c. 940 Ma, 1825 Ma and 2100-2560 Ma ; (ii) a granite boulder from a coarse-grained conglomerate yields a well-defined age of 582 ± 5 Ma and subordinated inherited ages between 1800 and 2200 Ma. Zircon rims of probable metamorphic origin provide a concordant age of 492 ± 4 Ma ; (iii) a gneissic band in the vicinity of the conglomerate is dated at 597 ± 4 Ma ; (iv) a coarse-grained garnet amphibolite yields an age of 517 ± 3 Ma interpreted as the emplacement age of the protolith, either as intrusive unit cutting accross the sedimentary succession or lava intercalated within the sediments.
The mainly Ediacarian record in the metasediments (quartzite and granite boulder in conglomerate) lead us to conclude that this material resulted from the erosion of a nearby Ediacarian (Cadomian ?) basement. The age of 517 Ma obtained on the amphibolite provides a minimum age for the sedimentary succession which deposition is therefore bracketed between 582 Ma and 517 Ma. This interval is comparable to that of the metasedimentary units of the Brioverian group of the Armorican Massif. Based on their low Th/U ratio, the 492 Ma-old zircon rims in the granite boulder are attributed to an Upper Cambrian metamorphic event.

Keywords: Western Alps / Briançonnais / Precambrian / Ediacarian / Alpin orogen / Cadomian orogen

Résumé – Découverte d'un socle édiacarien dans les Alpes occidentales : l'unité cristalline de Serre Chevalier (domaine briançonnais, France). Nous présentons de nouveaux âges U-Pb sur zircon (LA-ICP-MS) sur des roches cristallines variées localisées à Serre Chevalier au sein d'une unité de socle allochtone située au sommet de l'empilement de nappes de la zone briançonnaise ~ 5 km à l'ouest de la localité de Briançon. Cartographiée comme une unité métasédimentaire indifférenciée sur la carte géologique au 1/50 000^{e}, cet ensemble présente en fait une grande diversité lithologique, associant des micaschistes, des paragneiss, des quartzites, des conglomérats parfois très grossiers et des gneiss felsiques (leptynites) et mafiques (amphibolites) d'origine magmatique. Toutes les roches sont métamorphisées en lien avec un événement pré-alpin dans les conditions du faciès amphibolite et plus ou moins recristallisées dans les conditions du faciès amphibolite de bas degré à schiste vert lors d'un événement alpin. Les âges U/Pb sur zircon ont été obtenus sur 4 types de roches : (i) un quartzite micacé prélevé au cœur de l'unité métasédimentaire montre une population d'âges dominante vers 610 Ma, avec un âge minimal de 580 Ma, et des âges subordonnés à ~ 940 Ma, 1825 Ma et 2100-2560 Ma ; (ii) un bloc de granite extrait d'un

*Corresponding author: d.thieblemont@brgm.fr

conglomérat très grossier montre un âge bien défini à 582 ± 5 Ma et des âges subordonnés dans l'intervalle 1800-2200 Ma. Des surcroissances à la périphérie des zircons fournissent des âges à 492 ± 4 Ma ; (iii) une bande gneissique voisine du conglomérat fournit un âge à 597 ± 4 Ma ; (iv) un banc massif d'amphibolite à texture grossière est daté à 517 ± 3 Ma, âge interprété comme celui du protolithe, qui pouvait être un corps intrusif dans la série sédimentaire ou une lave intercalée dans les sédiments.
L'enregistrement essentiellement édiacarien dans les métasédiments (quartzite et bloc de granite dans le conglomérat), sans indice d'âge plus jeune, indique que ce matériel dérive de l'érosion d'un socle d'âge édiacarien (Cadomien ?). L'âge à 517 Ma obtenu sur l'amphibolite permet d'encadrer la mise en place de la série entre 582 Ma et 517 Ma ; cet âge est comparable à celui des séries métasédimentaires du Briovérien armoricain. Du fait de leur faible rapport Th/U, les surcroissances de zircon dans le bloc de granite sont attribuées à un événement métamorphique d'âge cambrien supérieur.

Mots-clés : Alpes occidentales / Briançonnais / Précambrien / Edicarien / Orogène Alpin / Orogène Cadomien

1 Introduction

The mainly Variscan age of the Alpine basement is widely documented and diverse models have been proposed trying to insert this prealpine basement in a plate tectonic model (see for example Guillot *et al.*, 2009; Guillot and Ménot, 2009; Faure and Ferrière, 2022; Von Raumer *et al.*, 2015 ; Ballèvre *et al.*, 2018, 2020; Siegesmund *et al.*, 2023; Jacob *et al.*, 2022; Vanardois *et al.*, 2022). This topic has led to the acquisition of a large amount of geochronological data by more and more precise techniques providing a large panel of ages indicating emplacement in the case of magmatic protoliths and source inheritance in the case of (meta)sedimentary rocks. To date, occurrences of Precambrian rocks have been recovered only in some places of the Central and Eastern Alps (see review in Von Raumer *et al.*, 2015 ; Siegesmund *et al.*, 2023). In the Western Alps, the possible occurrence of a Precambrian basement has been postulated in the 1970's based on field and petrographical considerations (Pêcher and Vialon, 1970) apparently supported by « total-Pb » zircon ages ranging from 430 to 800 Ma (Biju-Duval, 1975; Barféty and Pêcher, 1992). In particular, the occurrence of high-grade metamorphic rocks (granulite facies) in this basement was considered as a determining argument in favour of a pre-Hercynian age (Pêcher and Vialon, 1970). Recent work indicating an Ordovician age (c. 480 Ma) for granulite protolith and Carboniferous age for HT metamorphism (Jacob *et al.*, 2022) clearly discards the previous interpretation. In fact, the best argument for the possible occurrence of Precambrian rocks in the Western Alps is provided by the presence of Neoproterozoic zircons in metasedimentary formations thought to derive from the erosion of the pre-Alpine basement (Chu *et al.*, 2016; Fréville *et al.*, 2018). It has been shown that the pre-Alpine basement of the Central and Eastern Alps is partly made of an Ediacarian arc system (Von Raumer *et al.*, 2015), but no such basement has been evidenced to date in the Western Alps.

In this paper, we present new geochronological data obtained in a restricted crystalline terrain located in the Serre Chevalier area, about 5 km to the west of Briançon city. These data provide the first evidence of the existence of a Precambrian (Cadomian ?) event in the pre-Alpine basement of the Western Alps and its local reworking in a metasedimentary sequence of Brioverian (*i.e.*, Upper Ediacarian to lower Cambrian) age.

2 Geological outline

The studied area is located in the Briançonnais domain (simply named « Briançonnais » in the following text), one of the main tectonic domains of the internal Western Alps (Fig. 1).

At the latitude of Briançon (Figs. 1 and 2), a West-East section through the Alpine nappes stack cut accross the following domains: (i) the external Dauphinois domain which exposes a pre-Alpine basement (External Crystalline Massifs or ECM) covered by weakly to non metamorphosed Mesozoic to Cenozoic sedimentary series; (ii) the narrow Subbriançonnais unit which is bounded to the west by a major thrust (Frontal Penninic Thrust) putting the internal Alps in contact with the external Alps (Dauphinois); (iii) the Briançonnais which is a continental domain made of a stack of nappes with a lithostratigraphical succession clearly distinct from that of the Dauphinois; (iv) the Liguro-Piemontese domain, an ocanic domain including remnants of the original oceanic floor (ophiolites) and associated sediments (Schistes lustrés) intensively deformed and metamorphosed under high pressure – low temperature metamorphic conditions in the blueschist/eclogite facies (*e.g.* Bousquet *et al.*, 2012).

At the transition between the Briançonnais and Liguro-Piemontese domains a specific Piemontese domain is classically defined (Barféty *et al.*, 1995) which is considered as the continental margin making the transition between continent and ocean. Alternatively, this domain may be considered as part of the Briançonnais (Ballèvre *et al.*, 2020) with no need to define an additional paleogeographic domain. Following this point of view, we distinguish an external Briançonnais to the west and an internal Briançonnais to the east, the former being further divided into a western and an eastern subdomain (Barféty *et al.*, 1995; 1996).

The external Briançonnais, well exposed in the eponym Briançon region (Barféty *et al.*, 1995), is mainly characterized by well-developed Carboniferous to Permian sedimentary and volcano-sedimentary basins overlained by a thick Triassic sedimentary sequence, a restricted Jurassic to lower Cretaceous interval and an upper Cretaceous to Eocene sequence with dominant flysch deposits. The lowest term of the supracrustal succession is the Cristol detrital formation (conglomerates, sandstones) of supposed Namurian age (Barféty *et al.*, 1996). The basement below this formation is unknown. The whole domain is affected by west-verging

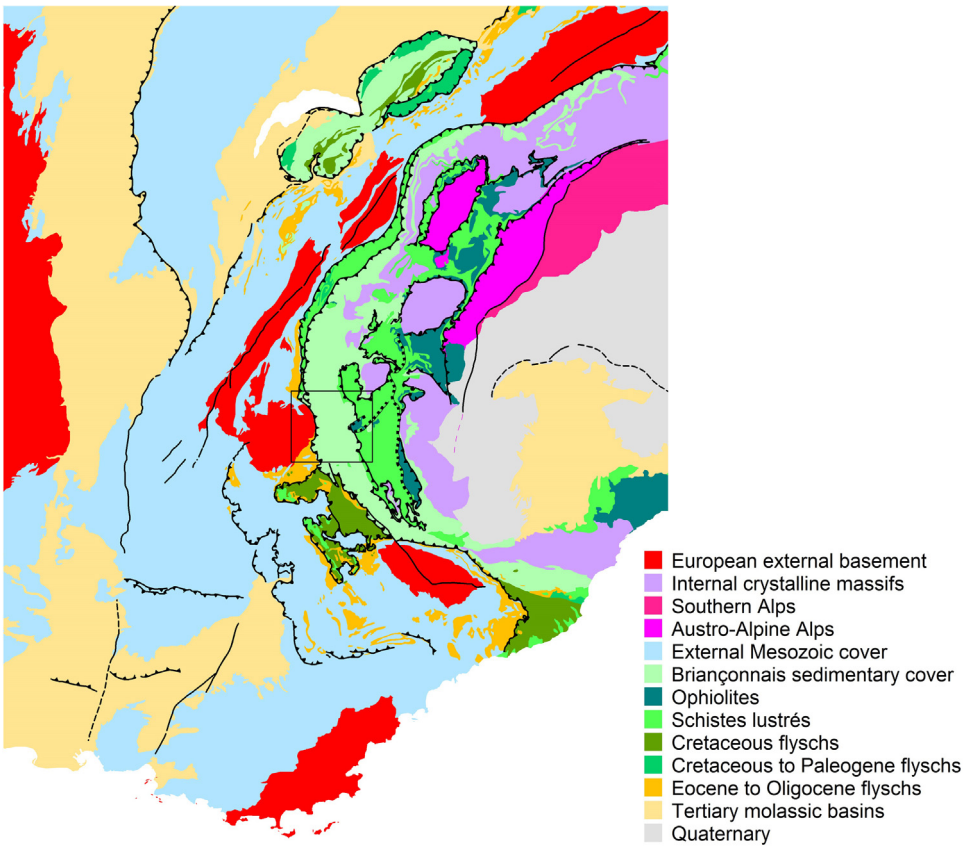

Fig. 1. Simplified geological of the Western Alps (modified from Chantraine *et al.*, 2003 after Schmid *et al.*, 2004 and Bousquet *et al.*, 2012) with indication of the location of the studied area (rectangle in the center of the figure).

thrusts and was metamorphosed under upper-greenschist facies conditions during the Eocene-Oligocene Alpine collision.

The internal (eastern) part of the Briançonnais domain, thrusted over the external one (Figs. 2 and 3Fig. 3), is dominated by east verging late stage backfolds and backthrusts that often invert the original nappe stack, bringing Briançonnais-derived thrust sheets over Liguro-Piemontese ophiolites and associated sediments (« schistes lustrés ») (Ballèvre *et al.*, 2020). The metamorphism is of blueschist facies with calculated temperature and pressure of 300°C and 6-10 kb respectively (Barféty *et al.*, 1995). The basement of the internal Briançonnais (*i.e.*, « Piemontese domain » according to Barféty *et al.*, 1995) is not visible in the Briançon region but may be observed to the north in Vanoise, being part of the group of the Internal Crystalline Massifs which represents the easternmost edge of the European basement (Fig. 1).

3 The Serre Chevalier crystalline terrain

For convenience the studied rocks are designated as the Serre Chevalier terrain but correspond to a group of three closely spaced outcrops of kilometric size (Fig. 2) designated by three different names (Eychauda, Crête du Mal Parti, Serre Chevalier) (Barféty *et al.*, 1996). These crystalline rocks are mapped as a unique formation on the geological map (symbol ξ) (Barféty *et al.*, 1996) but exhibit a large range of facies (see below) which could not be distinguished at the 1/50,000 scale (Barféty *et al.*, 1996). These outcrops are the largest though not the only occurrences of crystalline rocks in the external Briançonnais. Another one, located at the summit part of the Chaberton peak, is represented on Figures 2 and Figures 3. Other occurrences are of too limited extension to be reported on these figures. Collectively, they have been included in a specific lithotectonic unit considered as the uppermost part of the external Briançonnais nappes stack (Termier, 1903) now designated as the intermediate slices (Barféty *et al.*, 1995 and refs. therein). This situation is well exhibited in the Serre Chevalier area where the crystalline terrains lie at the top of the mountain range, a position placing them at the upper part of the nappes stack (Fig. 3).

To the east, the intermediate slices unit continues into the Prorel outcrop (Fig. 2) which is mainly composed of a coarse-grained and polygenic sedimentary breccia including crystalline fragments at the top (Barféty *et al.*, 1995). More to the east (Figs. 2 and 3), the intermediate slices unit marks the transition between the external and internal Briançonnais, being mapped as a west-verging tectonic slice backthrusted over the Triassic of the Chaberton peak on its eastern side (Fig. 3). The isolated outcrop of crystalline terrains mapped at the summit of that peak corresponds to the easternmost extension of the intermediate slices unit.

In the Serre Chevalier area (Fig. 4), the crystalline rocks reach an apparent maximal thickness of about 300 m and overlies different sedimentary units (Fig. 3) (Barféty *et al.*, 1996): a dark flysch (« flysch noir ») at the base, grading

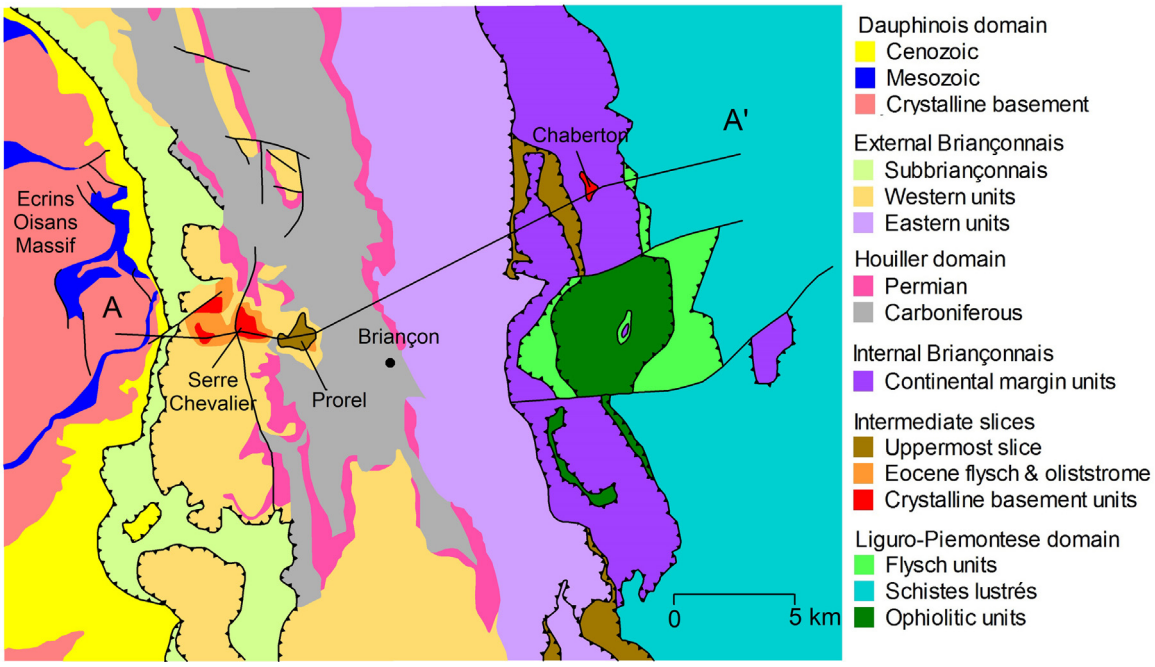

Fig. 2. Structural sketch map of the studied area (simplified from Barféty *et al.*, 1995) depicting the geological environment of the Serre Chevalier basement. For simplicity, the Subbriançonnais domain has been represented as part of the External Briançonnais. The A-A' line corresponds to the cross section exposed in Figure 3.

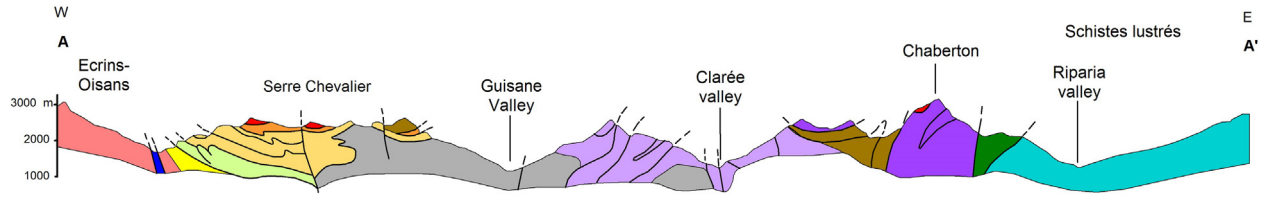

Fig. 3. W-E geological section accross the Alps at the latitude of Briançon (simplified from Barféty *et al.*, 1995). Legend as in Figure 2 except for the Houiller zone were Carboniferous and Permian are not distinguished.

upward into an olistostrome locally overlain by a polygenic breccia with abundant fragments derived from the overlying crystalline unit (Eychauda breccia, Fig. 4).

All those units have been proven to be in sedimentary contact (Barféty *et al.*, 1992; 1995). Microfossils at the base of the succession (dark flysch) have yielded a lower Bartonian age suggesting an upper Eocene age for the whole sequence (Barféty *et al.*, 1992). This led Barféty *et al.* (1992) to reinterpret the upper part of the Serre Chevalier succession as an olistostrome precursor to the emplacement of the intermediate slices and other Briançonnais nappes in a context of continental collision.

A more straightforward interpretation is to consider the intermediate slices unit as a unique olistostrome including a large range of olistoliths of either sedimentary or crystalline nature emplaced in the course of the dark flysch deposition. A Briançonnais origin would appear as the most probable for those olistoliths.

The Briançon geological map (1/50,000 scale) (Barféty *et al.*, 1995,1996) is the main document giving some information on the Serre Chevalier crystalline terrain and no additional work seems to have been published since that time. The unit is mapped as a composite formation associating dominant micaschist and other crystalline rocks with no atttempt to make cartographical distinctions between the different lithologies (Barféty *et al.*, 1996). It is described as a succession of micaschist and amphibolite beds with sparse lenses of orthogneiss, scarce pegmatites and also chlorite schists and dark schists. Massive amphibolites showing hornblende with brown core and barroisite rim are also described. Brown hornblende belongs to an early stage metamorphic assemblage also including garnet, brown and white mica, and rutile. Late stage minerals include green amphibole (barroisite), chlorite and white mica. Chlorite is frequently observed as pseudomorphs after biotite or garnet.

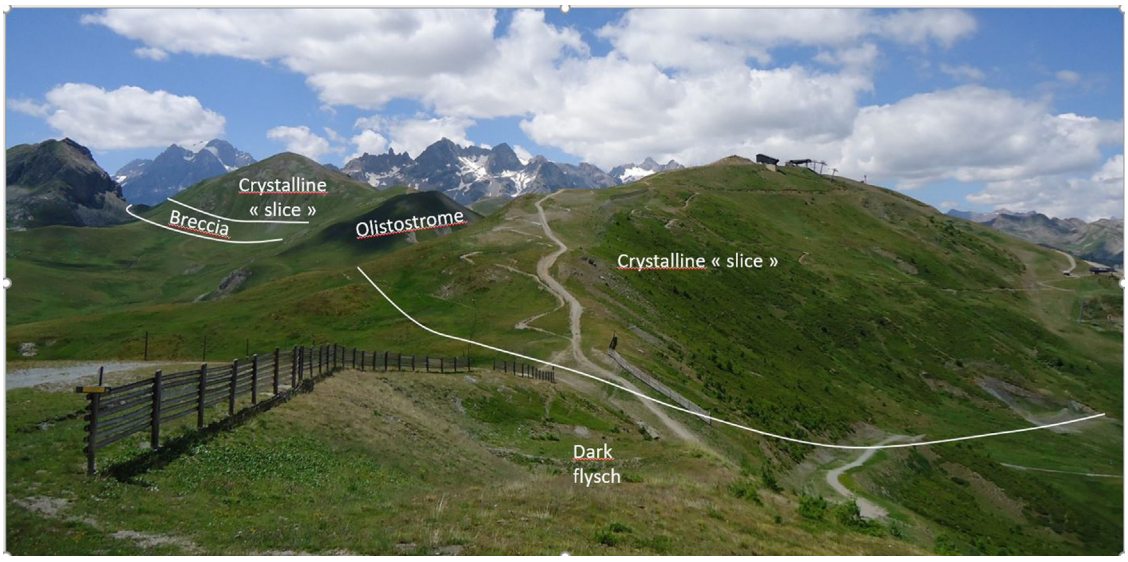

Fig. 4. Landscape of the Serre Chevalier ski station showing two of the three outcrops of crystalline rocks in this area. The Eocene olistostrome is intercalated between the two outcrops and the more distant one (Eychauda moutain) passes downward to a coarse-grained breccia mainly composed of crystalline fragments (Eychauda breccia).

Toward the base of the unit, a progressive mylonisation and retrogression affect the rocks with apparition of chlorite schists (Barféty *et al.*, 1995). Nevertheless, the contact with the basal breccia is described as stratigraphic. For instance, the retrogressed facies observed at the bottom of the basement unit also occur as blocks within the undelying breccia. This is one of the arguments which led Barféty *et al.* (1995) to conclude to an emplacement of the basement slices as olistoliths. After exhumation at surface, the basement has been fragmented and incorporated as blocks and panels of plurikilometric size in the Eocene sedimentary succession. For the authors, the metamorphism affecting the basement is clearly of ante-Permian age, but the retrogression could be related to exhumation and only barroisite may be considered as an alpine metamorphic mineral.

Our observations, including the petrographical study of representative facies (Supplementary materials, S1), are consistent with that of Barféty *et al.* (1996) with some significant additional observations. We do not attempt to draw a precise map as it probably requires to map at the 1/10,000 scale due to the short-scale transitions between lithologies.

The dominant lithologies are metasedimentary with a predominance of micaschist alternating with fine-grained gneiss richer in plagioclase. Transition may be gradual or sharp. In this latter case, gneiss occurs as distinct bands parallel to the main foliation. Quartzite may be locally abundant as submetric bands alternating with micaschist. Amphibolite and fine-grained felsic gneiss (leptynites) appear as decimetric to plurimetric bands (Fig. 5) intercalated within metasediments. Amphibolite and leptynite may alternate as very regular beds with sharp contacts. Amphibolite is generally coarse-grained with well visible amphibole and garnet. The textural association of these large secondary minerals is suggestive of a former subvolcanic (*i.e.*, doleritic) texture. A conglomeratic layer intercalated within the micaschists and paragneisses has also been observed (Fig. 6) with pebbles and boulders of granite some of them reaching an almost metric size.

Fig. 5. Outcrop of massive coarse-grained garnet amphibolite (sample BRI0057A).

This new investigation of the Serre Chevalier basement let us to select four rocks for a geochronological study: (i) a micaceous quartzite (sample BRI0321); (ii) a leptynite (fine-grained leucocratic gneiss) (sample BRI0058); (iii) a boulder of granite (sample BRI0334); (iv) a massive garnet-amphibolite (sample BRI0057A). Their petrographical descriptions and geographical coordinates are provided as Supplementary materials (Tab. S1).

4 Geochronological study

4.1 Analytical techniques

The sample preparation, including crushing, zircon extraction and thin section, has been operated in the BRGM laboratories (Orléans, France). In situ U-Pb analyses were

Fig. 6. Outcrop of metaconglomerate with schist and granite (blue circle) pebbles.

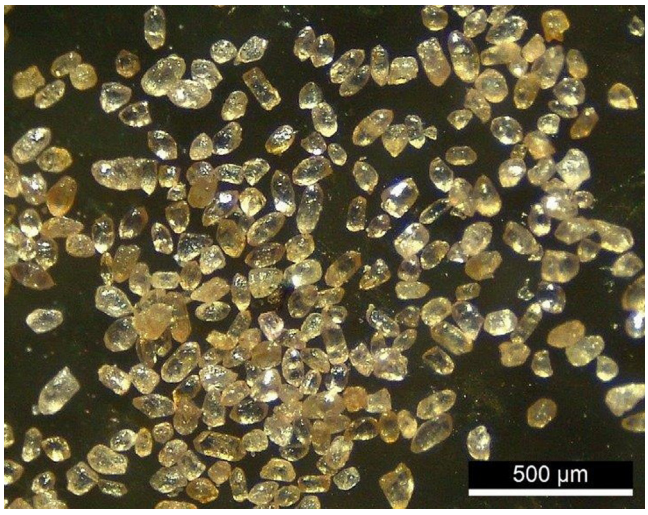

Fig. 7. Zircon population extracted from the BRI0321 sample observed with a binocular magnifier.

obtained on an Agilent 8900 ICP–MS for BRI0321 and BRI0057 and on ThermoScientific ICP-MS X séries II for BRI0058 and BRI0334, both coupled to a Cetac Excite 193nm laser ablation system. The sample is located in a dual-volume laser ablation cell with Helium gas flow. The detailed analytical parameters for the ICP-MS and the laser ablation system are listed in Table S2-1 (Supplementary materials).

The occurrence of common Pb in the sample can be monitored by the evolution of the ^{204}(Pb+Hg) signal intensity. No common Pb correction was applied. The ^{235}U signal is calculated from ^{238}U based on the ratio $^{238}U/^{235}U = 137.88$ for the analysis performed with XserieII spectrometer, but are directly measured with the Agilent 8900 spectrometer. Data were corrected for U–Pb and Th–Pb fractionation and for the mass bias by standard bracketing with repeated measurements of the 91500 zircon standard (Wiedenbeck *et al.*, 1995). Reproducibility and accuracy of the corrections are controlled through repeated measurements of the Plešovice zircon standard (338 ± 1 Ma, Sláma *et al.*, 2008) (Supplementary materials, Tab. S2-2 and Fig. S2). Data reduction was carried out with Gliter® (van Achterbergh *et al.*, 2001). Concordia ages and diagrams were generated using Isoplot/Ex version 4.15 (Ludwig, 2012). Uncertainties given in the Tables for individual analyses (ratios and ages) are at 2σ level. Results for age calculation and uncertainties are shown in the Figures at 2σ.

Concordance is calculated according to:
Conc = (Age $^{206}Pb/^{238}U$) X100/ (Age $^{207}Pb/^{235}U$).

The error correlation coefficient (ρ) is calculated according to Schmitz and Schoene (2007): $\rho_{R75\text{-}R68} = ((\sigma_{75}/R_{75})^2 + (\sigma_{68}/R_{68})^2 - (\sigma_{76}/R_{76})^2)/ (2*(\sigma_{75}/R_{75})*(\sigma_{68}/R_{68}))$ where $R75 = {}^{207}Pb/^{235}U$; $R68 = {}^{206}Pb/^{238}U$; $R76 = {}^{207}Pb/^{206}Pb$, σ = uncertainty of the isotopic ratio.

4.2 Results

Zircon cathodoluminescence images of all the dated zircons are provided as Supplementary materials (Figs. S3-1–Figs. S3-4). U/Pb analyses of the four studied samples are reported in Tables S4-1–S4-4.

4.2.1 Micaceous quartzite – Sample BRI0321

This sample shows a rather heterogeneous zircon population. Crystals are very small (< 100 µm), often broken (Fig. 7). They are colorless to pinky beige, translucent to opaque, subeuhedral to rounded. This wide diversity is consistent with the sedimentary nature of the sample. SEM image also reveals a highly heterogeneous zircon population in terms of zoning patterns, core-rim relationships, luminescence etc (supplementary materials, Fig. S3-1).

105 analyses have been performed on 105 zircons of varied shape and colour. These analyses show a large spread of ages between 500 and 3300 Ma (Fig. 8).

4 analyses are rejected because of a $^{206}Pb/^{204}Pb$ ratio lower than 1000 indicative of substantial common lead. 42 analyses are rejected for the statistics because they show a degree of discordance higher than 4%. A unique analyse attests for a very old age (> 3300 Ma). Age components deconvolution is done for the 58 remaining analyses using the Sambridge-Compston algorithm (Ludwig, 2012). The histogram (Fig. 9) indicates the existence of 5 populations. The younger one and most abundant (53% of the total) corresponds to an age of 610 ± 3

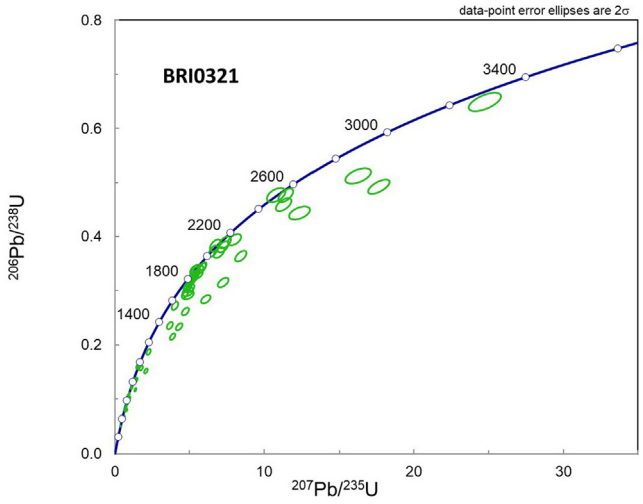

Fig. 8. Wetherill (1956) normal concordia diagram showing the U-Pb isotopic results of zircons from sample BRI0321 (micaceous quartzite).

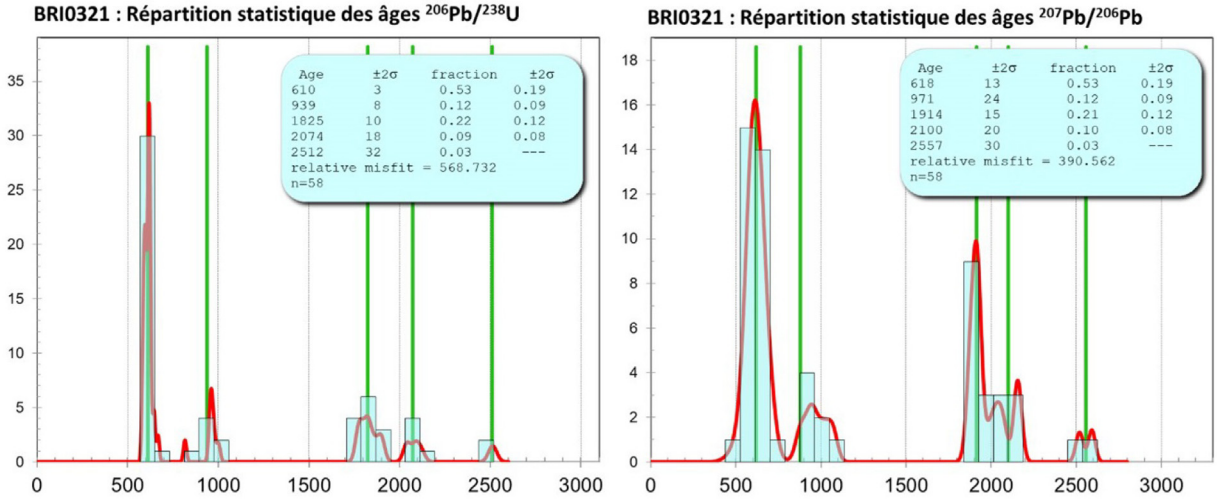

Fig. 9. Histograms and probability density plots of $^{206}Pb/^{238}U$ and ^{207}Pb-^{206}Pb ages in the BRI0321 sample.

Ma ($^{206}Pb/^{238}Pb$ ages) which indicates the predominance of Ediacarian elements amongst the source material. The youngest zircons are reported from three samples (BRI0321-6, BRI0321-26, BRI0321-91) which show $^{206}Pb/^{238}Pb$ ages in the range 580-584 Ma. An age of c. 580 Ma can therefore be considered as a maximum for the sedimentation of the quartzite. Note however that no age younger than Ediacarian is recorded. The four others age populations are grouped around 940 Ma (12% of the total), 1825 Ma (~ 20%), 2100 and 2560 (10% and 3% respectively) (Fig. 9).

4.2.2 Leptynite intercalated in paragneiss – Sample BRI0058

Because of the small size and scarcity of zircon, only about forty crystals have been extracted from this sample. Zircons are stubby, translucent, of pink color and slightly rounded. SEM image also reveals variable zoning patterns, core-rim relationships and luminescence intensities (Fig. 10).

30 analyses have been performed on 30 different crystals. 5 analyzed are rejected because of $^{206}Pb/^{204}Pb$ ratios < 800 indicating substantial common lead or excessive degree of discordance (*i.e.*, 10% tolerance for the $^{207}Pb/^{235}U$ vs. $^{206}Pb/^{238}U$ ages). Except for one spot (25) showing a concordant Paleoproterozoic age (c. 2090 Ma) (Fig. 11b), the 22 analyses plot along the concordia and amongst then 18 define a well-constrained age of 597 ± 4 Ma (Fig. 11).

4.2.3 Granite boulder – Sample BRI0334

This sample shows rare zircons of variable size (~100-500 μm) (Fig. 12). Crystals are generally stubby, light beige, translucent and euhedral to subhedral with frequent bubble inclusions and some of them (Supplementary materials, Fig. S3-3) exhibit a distinct core with an irregular shape and bright CL luminescence surrounded by a well-crystallized and oscillatory zoned rim with darker CL luminescence (Fig. 13).

45 analyses have been performed on 40 zircons. 4 analyses have been discarded because of a $^{206}Pb/^{204}Pb$ ratio lower than

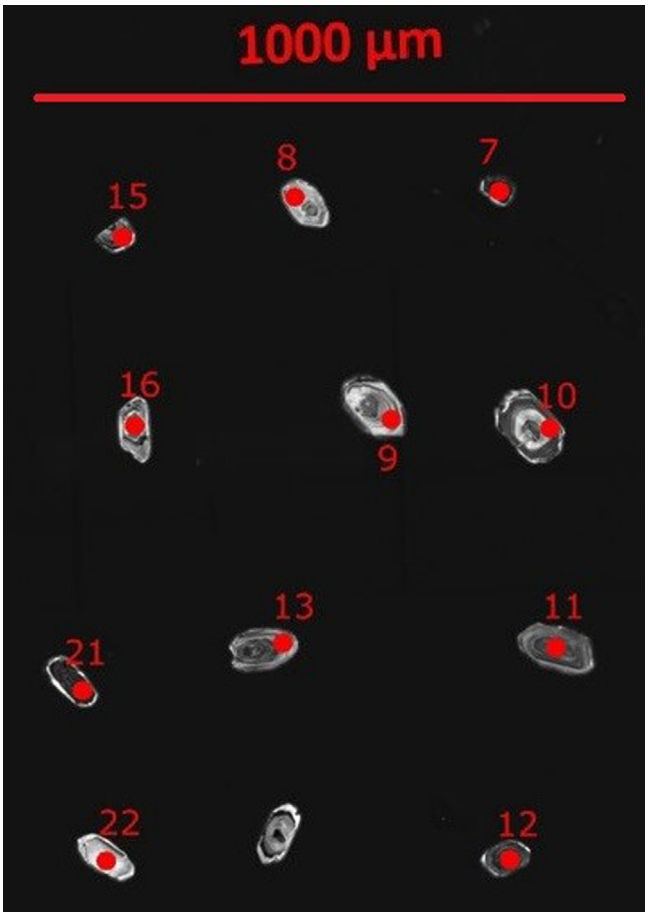

Fig. 10. Cathodoluminescence image of some zircons of the BRI0058 sample. The ages obtained at each spot are listed in Table S4-2 (Supplementary materials).

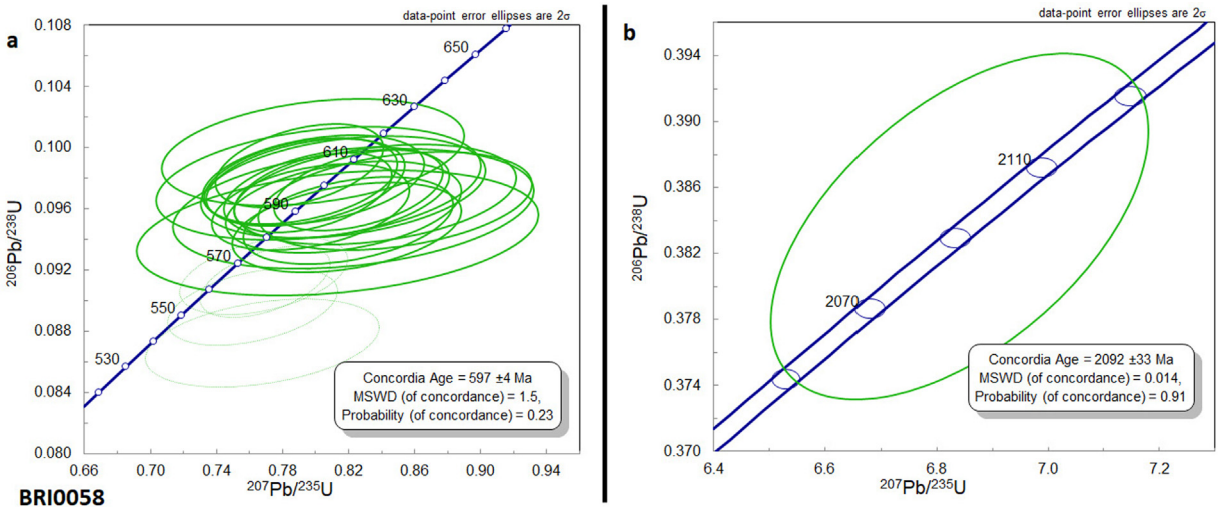

Fig. 11. Wetherill (1956) diagram for the analyses performed in sample BRI0058 (a) with emphasis on one concordant age giving an age around 2100 Ma (b).

Fig. 12. Zircons analyzed from the sample BRI0334 observed with a binocular magnifier.

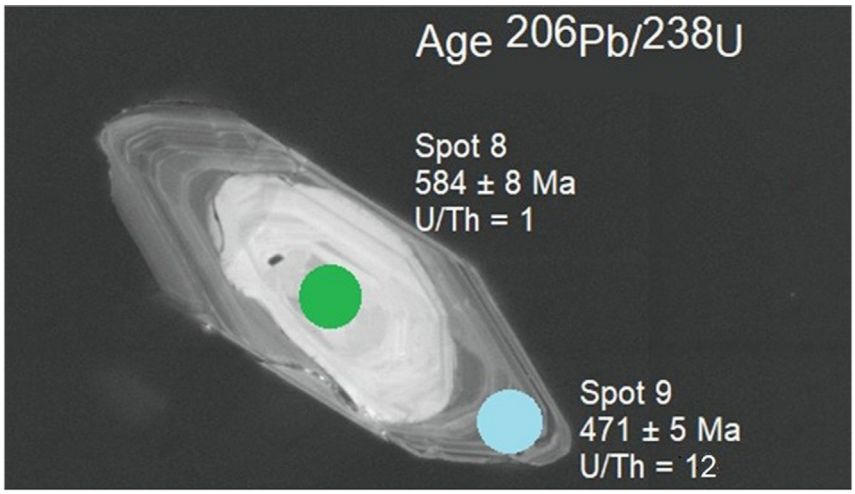

Fig. 13. Cathodoluminescence image of a representative zircon crystal from sample BRI0334, showing the typical core-rim relationship, with distinct $^{206}Pb/^{238}U$ ages and Th/U ratios obtained for spots 8 and 9 respectively in the core and rim of the zircon.

1000 indicative of substantial common lead. The remaining 41 analyses are very scattered in the Concordia diagram (Fig. 14a). 34 plots along the concordia between 750 and 400 Ma with two significant events at 580-600 Ma (13 analyses) and 490-500 Ma (18 analyses) (Fig. 14b). An age of 582 ± 5 Ma may be calculated from 5 concordant analyses of the first group (Fig. 15b) which corresponds mostly to crystal cores (spots 2, 7, 13, 25, 37) and display low U/Th ratios (< 5). An age of 492 ± 4 Ma may be calculated from 9 analyses of the second group (Fig. 15d) which correspond to crystal rims (spots 1, 4, 11, 29, 30, 34, 35, 38, 40) and display high U/Th ratios (> 5). Despite the mild accuracy of the probability associated with this age (MSWD = 5.4); the grouping of points confers it a reasonable level of confidence. An example is displayed on Figure 13, with a single zircon showing a core at 584 ± 8 Ma ($^{206}Pb/^{238}U$ age) and U/Th ratio of 1 and a rim at 471 ± 5 Ma and U/Th ratio of 12.

Plot of $^{206}Pb/^{238}U$ age against Th/U (Fig. 16) shows a clear discrimination between two groups : (i) a young group corresponding mostly to analyses performed at zircon rims. Except for 3 analyses, the zircons of this group show Th/U ratios < 0.15 and 11 out of them show Th/U < 0.1 ; (ii) an old group corresponding only to analyses performed in zircon cores. The Th/U ratio in this group ranges from 0.2 to 1 being generally higher than that of the other group. Note that all analyses with a Th/U ratio < 0.15 and age < 500 Ma are from the rims, nevertheless some zircons display rims with Th/U > 0.15 and age > 500 Ma. This indicates that young rims are not present around all zircons.

Differences of Th/U ratios between magmatic and metamorphic zircons have been frequently observed with the conclusion that magmatic zircon generally display high Th/U relative to metamorphic ones (Pystina and Pystin, 2019 and refs. therein). Based on a regional compilation of U-Th data from igneous and metamorphic zircons from Western Australia, Yakymchuk *et al.* (2018) showed that less than 1% of the igneous zircons from their data base display Th/U ratios < 0.1, whereas such low values are commonly observed in the

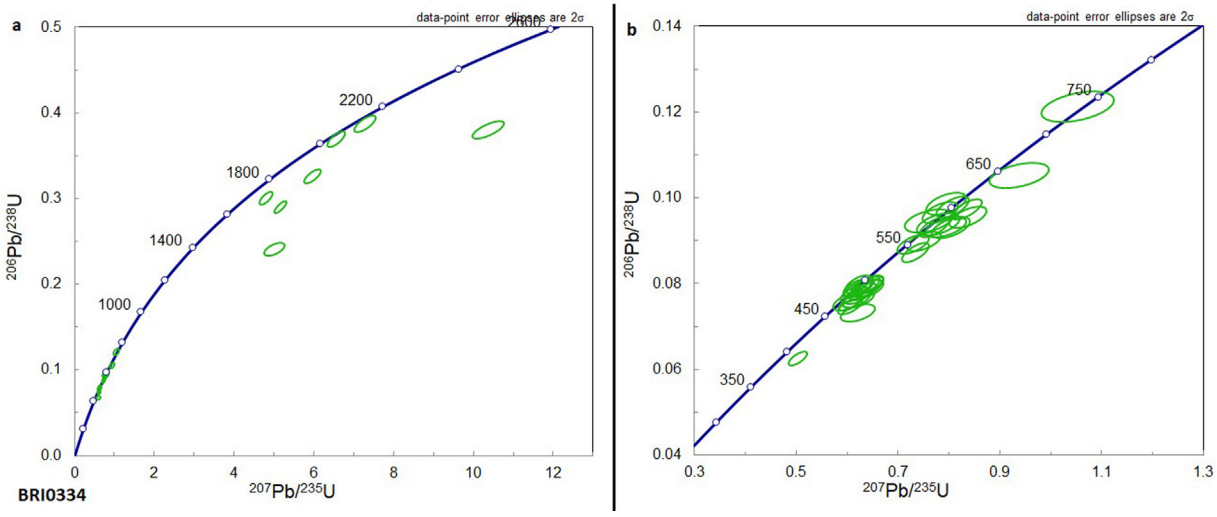

Fig. 14. Wetherill (1956) normal concordia diagram showing the entire set of U-Pb isotopic results obtained from sample BRI0334 (a) and focus on the lower part of the diagram (350-750 Ma interval) (b).

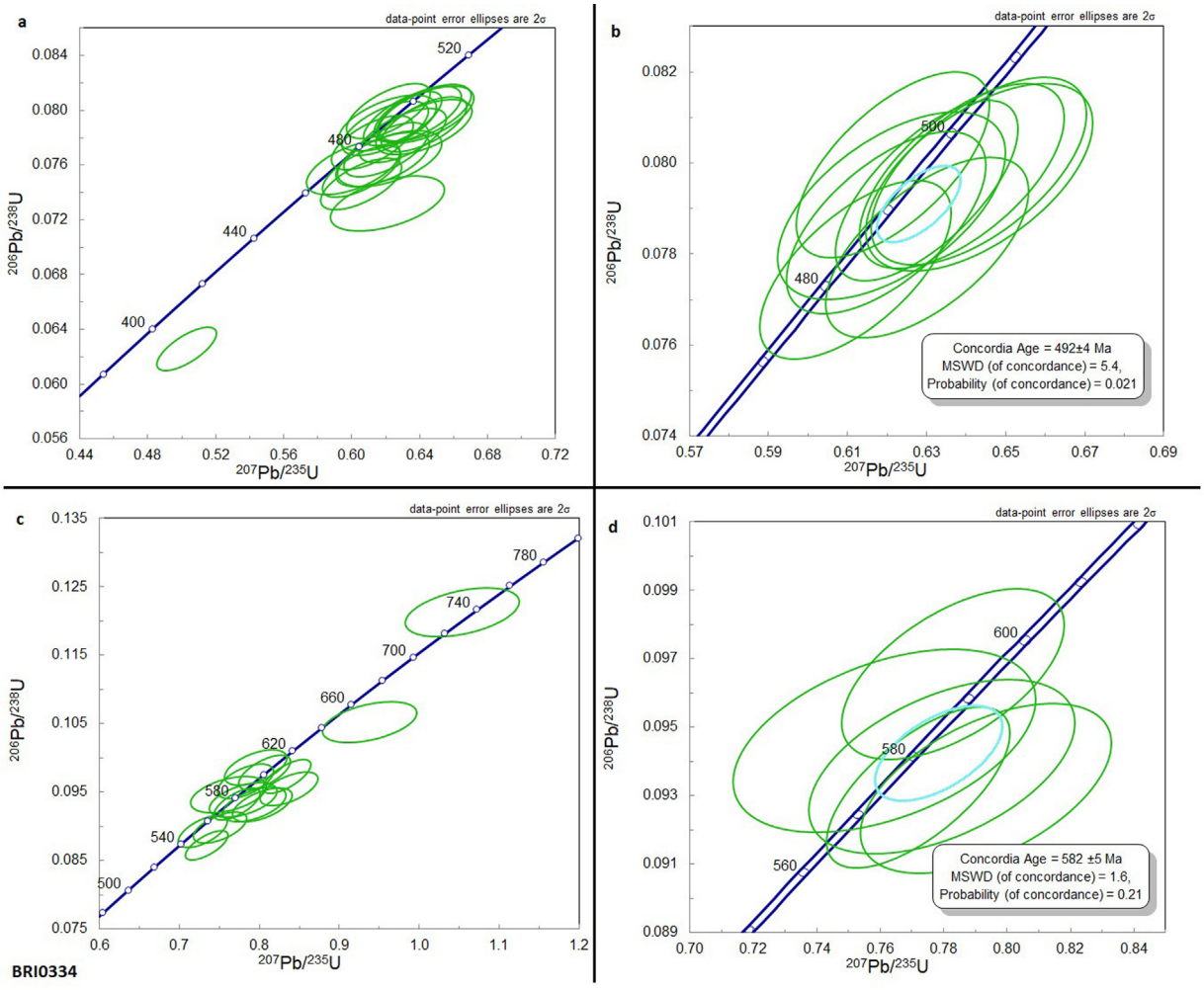

Fig. 15. Wetherill (1956) normal concordia diagram showing the U-Pb isotopic results obtained in sample BRI0334 in the ranges 380-520 Ma (a) and 500-780 Ma (c) with details of analyses around the two calculated ages at 492 Ma (b) and 582 Ma (d).

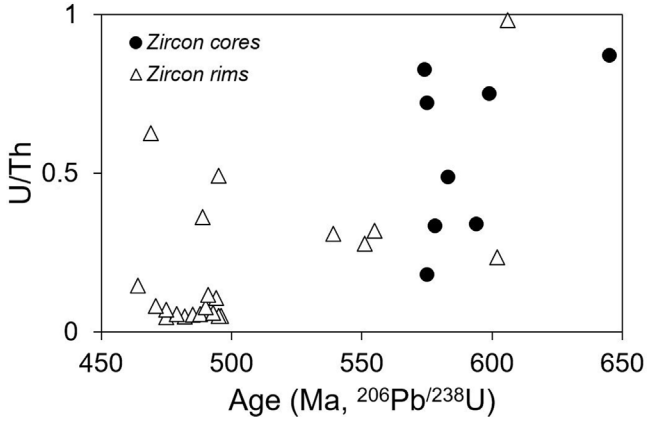

Fig. 16. Plot of Th/U ratio against $^{206}Pb/^{238}U$ age for the analyses performed in the zircons of sample BRI0334 with distinction between core and rim analyses.

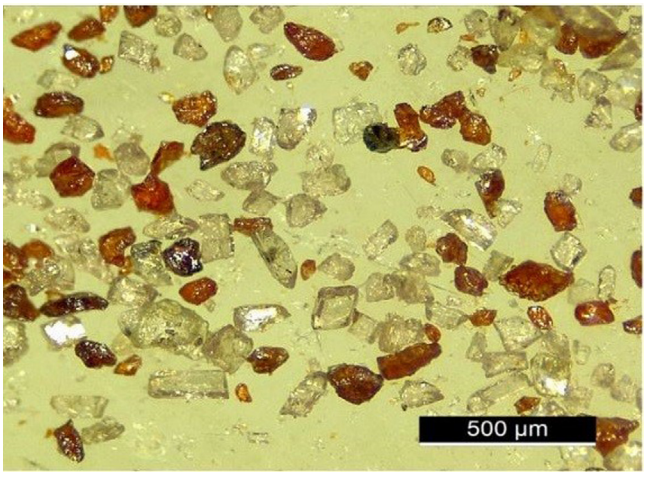

Fig. 17. Zircons (translucent) and rutile (brown to red) extracted from sample BRI0057A. Binocular magnifier view.

metamorphic zircons. Nevertheless, the rule is not absolute; an unambiguous example of igneous zircons with low Th/U ratios has been reported by Lopez-Sanchez *et al.* (2015). Those zircons of Permian occur as rims surrounding zircon cores of Ediacarian age.

According to Hoskin and Schaltegger (2003) rims could form in solid state by (re)crystallization or dissolution-precipitation in presence of a metamorphic fluid. Conversely data from Lopez-Sanchez *et al.* (2015) show that such rims may also result from crystallization at a magmatic stage.

Kirkland *et al.* (2015) proposed a method for relating measured zircon Th/U ratio to that expected for zircon crystallized in equilibrium with the host magmatic rock. The objective is to evaluate the consistency between the Th/U ratio of zircon and nature of the magmatic host rock. Calculation of zircon/whole rock fractionation factors of U and Th for a range of magmatic rocks of different temperatures indicates a decrease of the solubility of both elements in zircon at increasing temperature. The method of Kirkland *et al.* (2015) has been tested for the granite block BRI0334.

The geochemical analyse of BRI0334 (Supplementary materials, Tab. S5) indicates a moderate SiO_2 content (68.1%) and high TiO_2 content (= 0.74%) suggestive of relatively high temperature (*e.g.*, Hayden and Watson, 2007). U and Th contents are respectively of 2.13 ppm and 16.3 ppm. $U_{(zircon/whole\ rock)}$ and $Th_{(zircon/whole\ rock)}$ fractionation factors have been calculated for the two age-populations of zircons (492 Ma and 582 Ma) from the mean U and Th contents measured at each spot. $U_{(zircon/whole\ rock)}$ and $Th_{(zircon/whole\ rock)}$ for the young rims are of 317 and 3 respectively, against 259 and 15 for the c. 582 Ma-old zircons. Values for the rims would suggest a temperature of c. 800°C if calculated after U and more than 1200°C if estimated after Th. This is clearly inconsistent, indicating that zircons with the U and Th contents of zircon rims of BRI0334 cannot crystallize from a magma having the composition of BRI0334.

The temperature obtained from the mean U and Th contents of the c. 582 Ma-old zircons are of c. 850°C when calculated from U and c. 1000°C when calculated from Th. This is more consistent and shows that zircon with the U and Th contents of the c. 582 Ma-old zircons may actually crystallize from a magma having the composition of BRI0334. Note that the temperatures estimated for BRI0334 fom three different methods (zircon solubility, Watson and Harisson, 1983; rutile solubility, Hayden and Watson, 2007; monazite solubility, Montel, 1993) are similar and equal to 900°C.

4.2.4 Coarse-grained amphibolite – BRI0057A

The zircon extracted from this amphibolite are very small, brittle, translucent, of pale pink color and euhedral to anhedral (Fig. 17). Under CL images (Supplementary materials, Fig. S3-4) the zoning pattern of the grains is often "striped", diffuse or patchy, rather than clearly oscillatory. Such features are quite common in zircons from mafic rocks (Laurent *et al.*, 2017). Rutile has also been extracted but attempt to date it by LA-IC-MS technique was unsuccessfull due to very low U contents.

45 analyses have been performed on 38 zircons. 5 analyses are rejected from age calculation because of $^{206}Pb/^{204}Pb < 1000$ indicative of substantial common lead. 5 other analyses are rejected because of degrees of discordance > 4% (Fig. 18). Amongst the 35 remaining analyses, the 27 most concordant points give a concordia age of 517 ± 3 Ma interpreted as the crystallization age of the protolith.

5 Discussion

5.1 Chronology of the Serre Chevalier crystalline terrain

The results obtained on the micaceous quartzite BRI0321, with a well-defined age of 610 ± 3 Ma corresponding to more than half of the zircon population and a subordinate age of 939 ± 8 Ma, clearly point to the dominant contribution of Neoproterozoic material in the original sediment. Minimal ages of 580 Ma obtained from the zircons of this rock fixes a maximal age for the deposition of the original sediment.

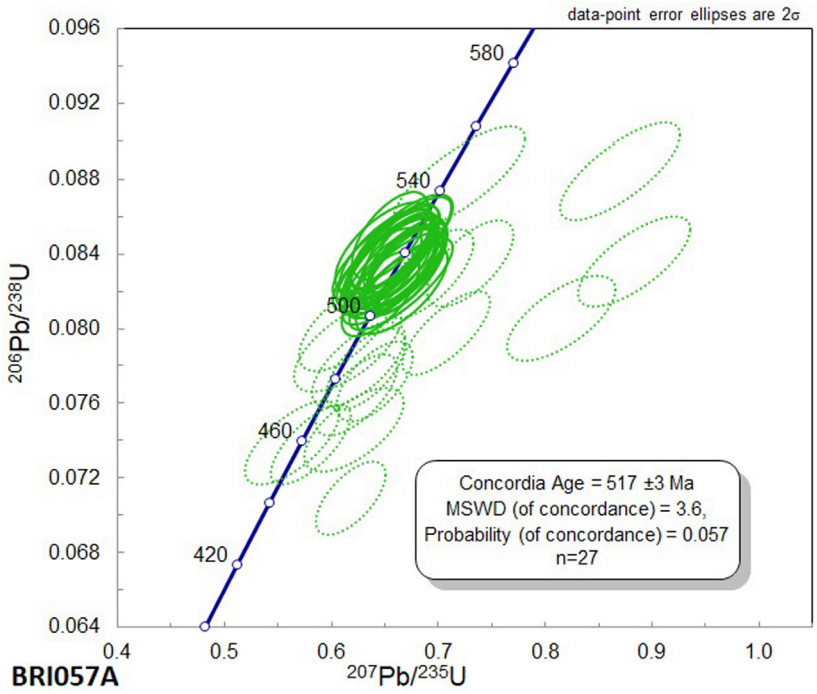

Fig. 18. Wetherill (1956) normal concordia diagram showing the U-Pb isotopic results obtained from the 45 zircon analyses performed in sample BRI0057A.

The quartzite alternates with the more common micaschist lithology which has not been analyzed but constitutes the matrix of the conglomerate with granitic pebbles, one of them (sample BRI0334) giving two main zircon ages populations: 492 ± 4 Ma and 582 ± 5 Ma.

As pointed earlier, the younger age is obtained from zircon rims which are clearly distinct from the core and present lower Th/U ratios (< 0.15). From this low Th/U ratio and considerations about the fractionation factors of U and Th relative to the host rock (granitic boulder BRI0334) we came to the conclusion that these rims cannot be of magmatic origin. We suggest that the zircon rims grown during a metamorphic event at 492 Ma, while zircon cores had crystallized at 582 Ma from the granitic magma.

Taken together, the maximal sedimentation age of 580 Ma obtained from the micaceous quartzite and the age of 582 Ma age obtained for the granitic boulder imply the deposition of the sedimentary to have occurred after ~ 580 Ma.

The wide spectrum of ages obtained for the micaceous quartzite attests for multiple sources. A dominant Ediacarian age is indicated by the well-defined peak at 610 ± 3 Ma. Another peak at 939 ± 8 Ma witnesses another Neoproterozoic contribution whereas the remaining zircon populations attest for Paleoproterozoic supplies.

The well-defined age of 597 ± 4 Ma obtained for the leptynite alternating with paragneiss, with only one analysis giving an older date of c. 2.1 Ga is again compatible with a Neoproterozoic age of the Serre Chevalier crystalline terrain. Two hypotheses may be envisaged: (i) the leptynite had a magmatic origin and emplaced as lava interbedded in the sedimentary sequence or as dyke cutting accross it; (ii) the leptynite derived from a sedimentary protolith and could correspond to an arkosic bed with a composition very close to that of its magmatic precursor. This latter hypothesis is the most consistent. Knowing that the maximal age of deposition of the sedimentary sequence is 580 Ma presence of a 597 Ma-old lava or intrusion in this sequence is actually inconsistent.

Another data to be discussed is the age of 517 ± 3 Ma obtained on the garnet-amphibolite BRI0057A. This rock is clearly of magmatic origin and intercalated within metasediments. Initial emplacement may have been extrusive (lava) or intrusive (lode). A volcanic origin would implie the deposition of the sedimentary series to have taken place at 517 Ma and an intrusive origin that it took place after 582 Ma and before 517 Ma. An intrusive origin is more compatible with the coarse texture of the amphibolite but this fact is not really conclusive. In the volcanic hypothesis, the lack of any zircon with age close to 517 Ma in the metasediments would implie the volcanic material to have never been reworked in the sediments. This is again more compatible with an intrusive origin but not totally conclusive. In any case the available constraints make sure that the emplacement of the Serre Chevalier unit occurred in the interval 582-517 Ma.

Finally, as discussed earlier, we interpret the 492 Ma age obtained on the zircon rims of the granite pebble BRI0334 as reflecting a later metamorphic event, which presumably affected the whole Serre Chevalier crystalline basement. Evidence of amphibolite-facies metamorphism is indeed found in several lithologies of the Serre-Chevalier unit. In particular, the mafic amphibolite (sample BRI0057A) displays a well-developed amphibolite-facies assemblage with coexistence of green hornblende, garnet and rutile. Considering the coeval

Table 1. Review of precise geochronologgical data for rocks dated at > 500 Ma in different areas of the Alps.

Location	Reference	Litholog	Method	System	Mineral	AGE	Error
External crystalline Massifs							
Chamrousse Ophiolite	Ménot R.P. *et al.* (1988)	Plagiogranite	TIMS Dissolution	U-pb	zircon	496	6
Chamrousse Ophiolite	Pin C., Carme F. (1987)	Métabsalte	Sm-Nd isochron	Sm-Nd	WR& mineral isochron	497	24
Briançonnais domain							
Ambin dome	Bertrand *et al.* (2000a)	Metarhyolite	SHRIMP	U-pb	zircon	500	8
Fibestre basement	Bertrand *et al.* (2000b)	Métagranophyre	TIMS Dissolution	U-pb	zircon	511	9
Bellecôte-Mont-Pourri	Guillot *et al.* (1991)	Granophyre	TIMS Dissolution	U-pb	zircon	507	9
Thyon métagranite	Bussy *et al.* (1996)	Orthogneiss	TIMS Dissolution	U-pb	zircon	500	+3/-4
Thyon métagranite	Scheiber *et al.* (2014)	Thyon Orthogneiss	LA-ICPMS	U-pb	zircon	505	4
Ergischhorn unit, gabbroic intrusion	Sartori *et al.* (2006)	Metaggabri (vein)		U-pb	zircon	504	2
Furgg zone							
Furgg Zone mafic rocks	Liati *et al.* (2001)	Amphibolitized eclogite	SHRIMP	U-pb	zircon	510	4
Lepontine Alps							
Biasca-Loderio maficultramafic unit	Schaltegger *et al.* (2002)	Amphibolite	TIMS Dissolution	U-pb	zircon	511	8
Biasca-Loderio maficultramafic unit	Schaltegger *et al.* (2002)	Amphibolite	SHRIMP	U-pb	zircon	518	11
Biasca-Loderio maficultramafic unit	Schaltegger *et al.* (2002)	Amphibolite	TIMS Dissolution	U-pb	zircon	519	39
Scheggia-Diorite	Bussien *et al.* (2011)	Scheggi-Diorite	LA-ICPMS	U-pb	zircon	533.5	7.4
Massari-Diorite	Bussien *et al.* (2011)	Massari-Diorite	LA-ICPMS	U-pb	zircon	544.1	4.5
Adula Nappe	Cavargna-Sani *et al.* (2015)	Amphibolite gneiss	TIMS Dissolution	U-pb	zircon	514.7	+2.6/-2.2
Adula Nappe	Cavargna-Sani *et al.* (2015)	Amphibolite gneiss	TIMS Dissolution	U-pb	zircon	517.1	+2/-3.7
Adula Nappe	Cavargna-Sani *et al.* (2015)	Kyanite eclogite	TIMS Dissolution	U-pb	zircon	521.1	+5/-4.3
Adula Nappe	Liati *et al.* (2009)	Orthogneiss	SHRIMP	U-pb	zircon	587	5
Adula Nappe	Liati *et al.* (2009)	Eclogite	SHRIMP	U-pb	zircon	595	9
Austroalpine domain							
Silvretta nappe mafic Complex	Schaltegger *et al.* (1997)	Metagabbro	TIMS Dissolution	U-pb	zircon	522	6
Silvretta nappe mafic Complex	Schaltegger *et al.* (1997)	Flasergabbro	TIMS Dissolution	U-pb	zircon	523	3
Silvretta nappe mafic Complex	Schaltegger *et al.* (1997)	Metatonalite	TIMS Dissolution	U-pb	zircon	524	6
Silvretta nappe mafic Complex	Schaltegger *et al.* (1997)	Metadiorite	TIMS Dissolution	U-pb	zircon	609	3
Silvretta nappe	Müller *et al.* (1996)	Plagiogranite	TIMS Dissolution	U-pb	zircon	532	30
Mönchalpgneiss, silvretta nappe	Poller (1997)	Gneiss	TIMS Dissolution	U-pb	zircon	528	
Tauern Window	kebede *et al.* (2005)	Gabbro clast in metaagglomerate	TIMS Dissolution	U-pb	zircon	536	8

stability of rutile and garnet, this metamorphism presumably occurred at relatively high pressure >10 kbar (Green *et al.*, 2016). This metamorphism is clearly pre-Alpine (*i.e.*, pre-Permian) (Barféty *et al.*, 1995) but remains to be precisely dated.

5.2 Regional perspective

Precambrian to lower Cambrian rocks are rather scarce in the Alpine basement. Occurrences of rocks older than 500 Ma listed in Table 1 show that they occur mainly in the Eastern and Central Alps. To our knowledge, the rocks of Serre Chevalier are the first Ediacarian formations dated so far in the Western Alps.

In the external crystalline Massifs (ECM), the oldest known formation is the ophiolite complex of Chamrousse which has been dated around 500 Ma (Ménot *et al.*, 1988; Pin and Carme, 1987) and is therefore significantly younger than the Serre Chevalier crystalline terrains.

In the Briançonnais domain, different occurrences of intrusive felsic rocks dated between c. 510 and 500 Ma are reported (Tab. 1). These veins cut accross metasedimentary sequences whose minimum deposit age is therefore of 510-500 Ma but no other geochronological constraints are available.

More to the east, data obtained in the Lepontine Alps and Austroalpine domain indicate the occurrence of a large set of metabasic rocks with ages between c. 540 and 500 Ma (Tab. 1) which have been interpreted as scattered relicts of former magmatic arcs of Ediacarian to Cambrian age (Von Raumer *et al.*, 2015). Precise ages older than 540 Ma are however rather scarce (Tab. 1) and obtained on particular samples of local occurrence.

A piece of basement comparable to the one we date in the Serre Chevalier area is therefore unknown in the Alpine context which makes impossible to correlate the Serre Chevalier with any geological unit around. Nevertheless, the occurrence of a Neoproterozoic basement is suspected in many places and consistent with the ages obtained to date on inherited zircons in some metasedimentary sequences (Fréville *et al.*, 2018 ; Chu *et al.*, 2016 ; Manzotti *et al.*, 2015, 2016) or on veins cutting accross them (see refs. in Tab. 1).

6 Conclusions and perspectives

The new results presented in this article provide the first occurrence of pre-Alpine basement-rocks of Ediacarian age in the Western Alps. Ediacarian ages are obtained on a boulder of granite in a coarse-grained conglomerate (582 ± 4 Ma) and in a micaceous quartzite (c. 580 Ma) and leptynitic gneiss (597 ± 4 Ma) where they correspond to maximal deposit ages with no evidence of younger ones. A minimum emplacement age is constrained by the date at 517 ± 3 Ma obtained on a coarse-grained garnet amphibolite intercalated in the metasediments. The interval of 582-517 Ma is comparable to that obtained for the metasedimentary units of the Brioverian group of the Armorican Massif (Chantraine *et al.*, 2001) suggesting a probable « Cadomian » origin for the Serre Chevalier unit.

Finally, an age of 492 ± 4 Ma obtained from zircon rims in a granite block included in a conglomerate is interpreted as the age of a late stage metamorphic event.

Beyond these results, many aspects of the Serre Chevalier basement remain to be studied: (i) a detailed geological mapping at 1/25,000 or even 1/10,000 scale would help to elucidate the exact nature of the original sedimentary series and a possible olistostrome origin suggests by the presence of large granitic boulders; (ii) a quantitative petro-structural investigation would enable the determination of the tectono-metamorphic evolution at the pre-Alpine and Alpine stages including the signification and extent of the upper Cambrian event detected in the granitic block ; (iii) regional comparisons are necessary to search for possible correlations between the Serre Chevalier terrain and other basement domains of the Alps.

Beyond the Alps, the place and signification of the Serre Chevalier unit must be envisaged in the frame of the whole Cadomian belt, that is an arc and back-arc system located at the northern margin of Gondwana during Ediacarian (*e.g.*, Linnemann *et al.*, 2007; Stampfli *et al.*, 2013; Couzinié *et al.*, 2017).

Acknowledgments. This work has been realized in the frame of the « Chantier Alpes et bassins périphériques » project as part of the RGF (« Référentiel Géologie de la France ») national program sponsored by BRGM. Oscar Laurent and an anonymous reviewer are kindly thanked for their constructive comments which lead to significant improvements in the final version.

Supplementary Material

S1 – Petrographical descriptions – Descriptions pétrographiques

S2 – Analytical techniques – Techniques analytiques
Table S2-1 – Summary of operating conditions for the LA-ICP-MS equipment for U-Pb zircon dating
Table S2-2 – U-Pb analyses of quality control on Plešovice zircon (Slama *et al.*, 2008)
Fig. S2 – Results of repeated measurements on the Plešovice zircon standard

S3 – Zircon cathodoluminescence images for the studied samples with location of all analytical spots
Fig. S3-1 – Location of analytical spots in the 105 zircons analyzed in sample BRI0321
Fig. S3-2 – Location of analytical spots in the 30 zircons analyzed in sample BRI0058
Fig. S3-3 – Location of analytical spots in the 40 zircons analyzed in sample BRI0334
Fig. S3-4 – Location of analytical spots in the 105 zircons analyzed in sample BRI0057A

S4 – U-Pb analyses – Analyses U-Pb
Table S4-1 – Analytical results obtained from the zircons of sample BRI0321. The analyses typed in italic are not taken into account because of high contents of common lead or degrees of discordance higher than 4%
Table S4-2 – Analytical results obtained from the zircons of sample BRI0058. The analyses typed in italic are not taken into account because of high contents of common lead or high degrees of discordance
Table S4-3 – Analytical results obtained from the zircons of sample BRI0334. The analyses typed in italic are not taken into account because of high contents of common lead or high degrees of discordance

Table S4-4 – Analytical results obtained from the zircons of sample BRI0057A. The analyses typed in italic are not taken into account because of high contents of common lead or high degrees of discordance

S5 – Geochemical analyse of the BRI0334 granite

The Supplementary Material is available at https://www.bsgf.fr/10.1051/bsgf/2023011/olm.

References

Ballèvre M, Manzotti P, Dal Piaz GV. 2018. Pre-Alpine (Variscan) inheritance: a key for the location of the future Valaisan Basin (Western Alps). Tectonics 37:789–817. https://doi.org/10.1002/2017TC004633.

Ballèvre M, Camonin A, Manzotti P, Poujol M. 2020. A step towards unraveling the paleogeographic attribution of pre-Mesozoic basement complexes in the Western Alps based on U-Pb geochronology of Permian magmatism. Swiss J Geosci 113: 12. https://doi.org/10.1186/s00015-020- 00367-1

Barféty J-C., Pêcher A, with the collaboration of: Bambrier A, Demeulemeester P, Fourneaux J-C., Poulain P-A.,Vernet J, Vivier G. 1992. Notice explicative de la feuille Saint-Christophe-en-Oisans à 1/50 000, Orléans : BRGM, 64 p.

Barféty JC, Tricart P, Jeudy de Grissac C. 1992. La Quatrième écaille près de Briançon (Alpes françaises) : un olistostrome précurseur de l'orogenèse pennique éocène. *CR Acad Sci* 314 (1): 71–76.

Barféty JC, Lemoine M, Mercier D, Polino R, Nievergelt P, Bertrand J *et al.*, 1996. Carte géol. France (1/50000), feuille Briançon (823). Orléans : BRGM. Notice explicative par J.C. Barféty, M. Lemoine, P.C. de Graciansky, P. Tricart, D. Mercier et coll, 1995, 180 p.

Barféty JC, Lemoine M, Graciansky, Tricart P, Mercier D, avec la collaboration de Pêcher A *et al.*, 1995. Notice explicative, Carte géol. France (1/50000), feuille Briançon (823). Orléans : BRGM, 180 p. Carte géologique par J.C. Barféty, M. Lemoine, D. Mercier, R. Polino, P. Nievergelt, J. Bertrand, T. Dumont, S. Amaudric du Chaffaut, A. Pêcher, G. Monjuvent (1996).

Bertrand J-M., Pidgeon RT, Leterrier J, Guillot F, Gasquet D, Gattiglio M. 2000a. SHRIMP and IDTIMS U-Pb zircon ages of the pre-Alpine basement in the Internal Western Alps (Savoy and Piemont). *Bull Suisse Minéral Pétrogr* 80: 1–24.

Bertrand J-M., Guillot F, Leterrier J. 2000b. Âge Paléozoïque inférieur (U-Pb sur zircon) de métagranophyres de la nappe du Grand Saint-Bernard (zona interna, vallée d'Aoste, Italie). *C R Acad Sci Paris* 330: 473–478.

Biju-Duval J. 1975. Etude pétrologique des terrains cristallins de la région du Sirac (sud du massif des Ecrins-Pelvoux-Haut dauphiné) – Alpes-France. Thèse de doctorat. Université Joseph-Fourier-Grenoble I.

Bousquet R, Oberhänsli R, Schmid SM, Berger A, Wiederkehr M, Robert C *et al.*, 2012. Metamorphic framework of the Alps, Commission for the Geological Map of the World.

Bussien D, Bussy F, Magna T, Masson H. 2011. Timing of Palaeozoic magmatism in the Maggia and Sambuco nappes and paleogeographic implications (Central Lepontine Alps). Swiss J Geosci 104: 1–29. https://doi.org/10.1007/s00015-010- 0049-6

Bussy F, Derron M-H., Jacquod J, Sartori M, Thelin P. 1996. The 500 Ma-old Thyon metagranite: a new A-type granite occcurrence in the western Penninic Alps (Wallis, Switzerland). *Eur J Mineral* 8: 565–575.

Cavargna-Sani M, Epard JL, Bussy F, Ulianov A. 2014. Basement lithostratigraphy of the Adula nappe: implications for Palaeozoic evolution and Alpine kinematics. *Int J Earth Sci* (Geol Rundsch) 103: 61–82. https://doi.org/10.1007/s00531-013- 0941-1.

Chantraine J, Autran A, Cavelier C. 2003. Carte géologique de la France à l'échelle du millionième, 6^{e} édition bis, BRGM.

Chantraine J, Egal E, Thiéblemont D, Le Goff E, Guerrot C, Ballèvre M *et al.*, 2001. The Cadomian active margin (North Armorican Massif, France): a segment of the North Atlantic Panafrican belt. *Tectonophysics* 331: 1–18.

Chu Y, Lin W, Faure M, Wang Q. 2016. Detrital zircon U-Pb ages and Hf isotopic constraints on the terrigeneous sediments of the western Alps and their paleogeographic implications. *Tectonics* 35:1–20. https://doi.org/10.1002/2016 CT004276.

Couzinié S, Laurent O, Poujol M, Mintrone M, Chelle-Michou C, Moyen J-F *et al.*, 2017. Cadomian S-type granites as basement rocks of the Variscan belt (Massif Central, France): Implications for the crustal evolution of the north Gondwana margin. *Lithos* 286-287: 16–34.

Faure M, Ferrière J. 2022. Reconstructing the Variscan terranes in the Alpine basement: facts and arguments for an Alpidic orocline. *Geosciences* 12: 65:1–29. https://doi.org/10.3390/geosciences12020065.

Fréville K, Trap P, Faure M, Melleton J, Xian-Hua L, Wei L *et al.*, 2018. Structural, metamorphic and geochronological insights on the Variscan evolution of the Alpine basement in the Belledonne Massif (France). *Tectonophysics* 726: 14–42. https://doi.org/10.1016/j.tecto.2018.01.017.

Green ECR, White RW, Diener JFA, Powell R, Holland TJB, Palin RM. 2016. Activity-composition relations for the calculation of partial melting equilibira in metabasic rocks. *J Metam Geol* 92: 1181–1189.

Guillot F, Liégeois J-P., Fabre J. 1991. Des granophyres du Cambrien terminal dans le Mont Pourri (Vanoise, zone briançonnaise) : première datation U-Pb sur zircon d'un socle des zones internes des Alpes françaises. *C R Acad Sci Paris* 313(II): 239–244.

Guillot S, Ménot RP. 2009. Paleozoic evolution of the external crystalline massifs of the Western Alps. *CR Geosci* 341: 253–265.

Guillot S, di Paola S, Ménot RP, Ledru P, Spalla M, Gosso G *et al.*, 2009. Suture zones and importance of strike-slip faulting for Variscan geodynamic reconstructions of the External Crystalline Massifs of the Western Alps. *Bull Soc Géol Fr* 180: 483–500.

Hayden LA, Watson EB. 2007. Rutile saturation in hydrous melts and its bearing on Ti-thermometry of quartz and zircon. *Earth Planet Sci Lett* 258: 561–568.

Hoskin PWO, Schaltegger U. 2003. The composition of zircon and igneous and metamorphic petrogenesis. *Rev Mineral Chem* 53: 27–62.

Jacob JB, Janots E, Guillot S, Rubatto D, Fréville K, Melleton J *et al.*, 2022. HT overprint of HP granulites in the Oisans-Pelvoux massif: implications for the dynamics of the Variscan collision in the external Western Alps. *Lithos* 416-417: 1–23.https://doi.org/10.1016/j.lithos.2022.106650

Kebede T, Klötzli U, Kosler J, Skiöld T. 2005. Understanding the pre-Variscan and Variscan basement components of the central Tauern Window, Eastern Alps (Austria): constraints from single zircon U-Pb geochronology. *Int J Earth Sci (Geol Rundsch)* 94: 336–353. https://doi.org/10.1007/s00531-005-0487-y.

Kirkland CL, Smithies RH, Taylor RJM, Evans N, McDonald B. 2015. Zircon Th/U ratios in magmatic environs. Lithos 212–215: 397-414. http://dx.doi.org/10.1016/j.lithos.2014.11.021.

Laurent O, Couzinié S, Zeh A *et al.*, 2017. Protracted, coeval crust and mantle melting during Variscan late-orogenic evolution: U-Pb dating in the eastern French Massif Central. *Int J Earth Sci (Geol*

Rundsch) 106: 421–451. https://doi.org/10.1007/s00531-016-1434-9.

Liati A, Gebauer D, Mark Fanning C. 2009. Geochronological evolution of HP metamorphic rocks of the Adula nappe, Central Alps, in pre-Alpine and Alpine subduction cycles. *J Geol Soc London* 166: 797–810. https://doi.org/10.1144/0016-76492008-033.

Liati A, Gebauer D, Froitzheim N, Mark Fanning C. 2001. U-Pb SHRIMP geochronology of an amphibolitized eclogite and an orthogneiss from the Furg zone (Western Alps) and implications for its geodynamic evolution. *Schweis Mineral Petrogr Mitt* 81: 379–393. https://doi.org/10.5169/seals-61699.

Linnemann U, Gerdes A, Drost K, Buschmann B. 2007. The continuum between Cadomian orogenesis and opening of the Rheic Ocean: Constraints from LA-ICPMS U-Pb zircon dating and analysis of plate-tectonic setting (Saxo-Thuringian zone, north-eastern Bohemian Massif, Germany). In Linnemann U, Nance RD, Kraft P, Zulauf G. eds. *The evolution of the Rheic Ocean: from Avalonian Cadomian active margin to Alleghenian-Variscan collision*. Geol Soc Am Sp Paper 423: 61–96.

Lopez-Sanchez MA, Aleinikoff JN, Marcos A, Martínez FJ, Llana-Fúnez S. 2015. An example of low-Th/U zircon overgrowths of magmatic origin in a late orogenic Variscan intrusion: the San Ciprián massif (NW Spain). *J Geol Soc* 173: 282–291. https://doi.org/10.1144/jgs 2015-071.

Ludwig KR. 2012. ISOPLOT a geochronological toolkit for Microsoft Excel, Berkeley Geochronology Center, Spec. Pub. N° 5.

Manzotti P, Ballèvre M, Poujol M. 2016. Detrital zircon geochronology in the Dora-Maira and Zone Houillère: a record of sediment travel paths in the Carboniferous. Terra Nova 28: 279–288. https://doi.org/10.1111/ter.12219.

Manzotti P, Poujol M, Ballèvre M. 2015. Detrital zircon geochronology in blueschist-facies meta-conglomerates from the Western Alps: implications for the late Carboniferous to early Permian palaeogeography. *Int J Earth Sci (Geol Rundsch)* 104: 703–731. https://doi.org/10.1007/s00531-014- 1104-8.

Ménot RP, Peucat JJ, Scarenzi D, Piboule M. 1988. 496 My age of plagiogranites in the Chamrousse ophiolite complex (external crystalline massifs in the French Alps): evidence of a Lower Paleozoic oceanization. *Earth Planet Sci Lett* 88: 82–92. https://doi.org/10.1016/0012-821X(88) 90048-9.

Montel JM. 1993. A model for monazite/melt equilibirum and application to the generation of granitic magmas. *Chem Geol* 110: 127–146.

Müller B, Klötzli U, Schaltegger U, Flisch M. 1996. Early Cambrian oceanic plagiogranite in the Silvretta nappe eastern Alps: geochemical, zircon U-Pb and Rb-Sr data from garnet-hornblende-plagioclase gneisses. *Geol Rundsch* 85: 822–831.

Pêcher A, Vialon P. 1970. Présence de gneiss du faciès granulite dans le noyau précambrien du massif des Ecrins-Pelvaoux (Alpes du Dauphiné, France). *CR Acad Sc Paris* 270: 666–668.

Pin Ch, Carme F. 1987. A Sm-Nd isotopic study of 500 Ma old oceanic crust in the Variscan belt of western Europe: the Chamrousse ophiolite complex, Western Alps (France). *Contrib Mineral Petrol* 96: 406–413.

Poller U. 1997. U-Pb single zircon study of a gabbroic and granitic rocks of Val Barlas-ch (Silvretta nappe, Swizerland). *Schweis Mineral Petrogr Mitt* 78: 383–395. doi.org/10.5169/seals- 58490.

Pystina Y, Pystin A. 2019. Th/U relations as an indicator of the genesis of metamorphic zircons (on the example of the north of the Urals). In: Glagolev S, ed. ICAM 2019, SPEES pp. 129–132. https://doi. org/10. 1007/978-3-030-22974-0_30.

Schaltegger U, Nägler ThF, Corfu F, Maggeti M, Galetti G, Stosch HG. 1997. A Cambrian island arc in the Silvretta nappe: constraints from geochemistry and geochronology. *Schweiz Mineral Petrogr Mitt* 77: 337–350.

Schaltegger U, Gebauer D, von Quadt A. 2002. The mafic-ultramafic rock association of Loderio-Biasca (lower Pennine nappes, Ticino, Switzerland): Cambrian oceanic magmatism and its bearing on early Paleozoic paleogeography. *Chem Geol* 186: 265–279.

Scheiber T, Berndt J, Mezger K, Pfiffner OA. 2014. Precambrian to Paleozoic zircon record in the Siviez-Mischabel basement (western Swiss Alps). *Swiss J Geosci* 107: 49–64.

Schmid SM, Fügenschuh B, Kissling E, Schuster R. 2004. Tectonic map and overall architecture of the Alpine orogen. *Eclog Geol Helvet* 97: 93–117.

Schmitz MD, Schoene B. 2007. Derivation of isotope ratios, errors, and errors correlations for U-Pb geochronology using ^{205}Pb-^{235}U-(^{233}U)-spiked isotope dilution thermal ionization mass spectrometric data. *Geochem Geophys Geosyst* Q08006:1–20. https://doi.org/10.1029/2006 GC001492.

Siegesmund S, Oriolo S, Broge A, Hueck M, Lammerer B, Basei MAS *et al.*, 2023. Cadomian to Cenerian accretionary orogenic processes in the Alpine basement: the detrital zircon archive. *Int J Earth Sci*. 112:1157–1174. https://doi.org/10.1007/s00531-023- 02305-6.

Sláma J, Košler J, Condon DJ, Crowey JL, Gerdes A, Hanchar JM *et al.*, 2008. Plešovice zircon – a new natural reference material for U-Pb and Hf isotopic microanalysis. *Chem Geol* 249: 1–35. https://doi.org/10.1016/j.chemgeo.2007.11.005.

Stampfli GM, Hochard C, Vérard C, Wilhem C, von Raumer J. 2013. The formation of Pangea. *Tectonophysics* 593: 1–19.

Termier P. 1903. Les montagnes entre Briançon et Vallouise. *Mém Expl Carte Géol Fr* 182.

Van Achterbergh E, Ryan C, Jackson S, Griffin WL. 2001. Appendix 3 data reduction software for LA-ICP-MS in Laser-Ablation-ICPMS in the earth sciences. In : Sylvester P. ed. Mineral Ass Canada Short Course 29: 239–243.

Vanardois J, Trap P, Roger F, Melleton J, Marquer D, Paquette JL et al. 2022. Deformation, crustal melting and magmatism in the crustal-scale East-Variscan Shear Zone (Aiguilles-Rouges and Mont-Blanc massifs, Western Alps). J. Struct. Geol 163: 1-22. https://doi.org/10.1016/j.jsg.2022.104724.

Von Raumer J, Stampfli GM, Arenas R, Sánchez Martínez S. 2015. Ediacaran to Cambrian oceanic rocks of the Gondwana margin and their tectonic interpretation. *Int J Earth Sci* 104: 1107–1121. https://doi.org/10.1007/s00531-015-1142-x.

Watson EB, Harrison TM. 1983. Zircon saturation revisited: temperature and composition effects in a variety of crustal magma types. *Earth Planet Sci Lett* 64: 295–304. https://doi.org/10.1016/0012-821X(83)90211-X.

Wetherill GW. 1956. Discordant uranium-lead ages 1. *Trans Am Geophys Union* 37: 320–326.

Wiedenbeck M, Allé P, Corfu F, Griffin WL, Meier M, Oberli F *et al.*, 1995. Three natural zircon standards for U-Th-Pb, Lu-Hf, trace element and REE analysis. *Geostandards Newsletter* 19: 1–23.

Yakymchuk C, Christopher L, Kirkland CL, Clark C. 2018. Th/U ratios in metamorphic zircon. J Metamorph Geol 36: 715–737. https://doi.org/10.1111/jmg.12307.

Cite this article as: Thiéblemont D, Jacob J-B, Lach P, Guerrot C, Leguérinel M. 2023. First report of an Ediacarian basement in the Western Alps: the Serre Chevalier crystalline unit (Briançonnais domain, France), *BSGF - Earth Sciences Bulletin* 194: 16.